Advances in GEOPHYSICS

VOLUME 31

Advances in
GEOPHYSICS

Edited by

BARRY SALTZMAN

Department of Geology and Geophysics
Yale University
New Haven, Connecticut

VOLUME 31

ACADEMIC PRESS, INC.
Harcourt Brace Jovanovich, Publishers

San Diego New York Berkeley Boston
London Sydney Tokyo Toronto

ACADEMIC PRESS, INC.
San Diego, California 92101

United Kingdom Edition published by
ACADEMIC PRESS LIMITED
24-28 Oval Road, London NW1 7DX

LIBRARY OF CONGRESS CATALOG CARD NUMBER: 52-12266

ISBN 0-12-018831-7 (alk. paper)

PRINTED IN THE UNITED STATES OF AMERICA
89 90 91 92 9 8 7 6 5 4 3 2 1

CONTENTS

Hydrostatic Airflow over Mountains

RONALD B. SMITH

The Forcing and Maintenance of Global Monsoonal Circulations: An Isentropic Analysis

DONALD R. JOHNSON

HYDROSTATIC AIRFLOW OVER MOUNTAINS

RONALD B. SMITH
Department of Geology and Geophysics
Yale University
New Haven, Connecticut 06520

1. INTRODUCTION

The flow of a density stratified fluid over an obstacle has been widely studied because of its application to atmospheric airflow over the irregular terrain of the earth's surface. One particular problem of this type—steady, Boussinesq, hydrostatic, nonrotating flow, unbounded above—has emerged as a "classical" problem in this field of study. Its solutions are relevant to a variety of mountains with horizontal scales from 1 to 100 km (depending on wind speed). Furthermore, in spite of the small number of control parameters, these flows exhibit many interesting phenomena. Restricting attention to this problem eliminates certain aspects of mountain airflow theory, i.e. trapped lee waves, mountain wave amplification aloft, and Coriolis force–induced vortices (see the broader reviews in Smith, 1979; GARP, 1980), but retains a rich set of fluid dynamic processes with direct application to the atmosphere.

In this article, the theoretical research of the last 10 years on stratified flow over mountains is reviewed. Theories of vertically propagating waves, wave breaking, flow splitting, and wake eddies are discussed. Current knowledge of these phenomena is used to construct an approximate regime diagram depicting how the nature of mountain-induced flow disturbance depends on the control parameters of the problem. Atmospheric applications of recent theories are discussed and unsolved problems are identified.

1.1. Governing Equations

The starting point for this discussion is the set of governing equations for a stratified Boussinesq fluid:

$$\rho_0 \frac{D\mathbf{u}}{Dt} = -\nabla p - \rho g \mathbf{k} + \mu \nabla^2 \mathbf{u} \tag{1}$$

$$\nabla \cdot \mathbf{u} = 0 \tag{2}$$

$$\frac{D\rho}{Dt} = \kappa \nabla^2 \rho \tag{3}$$

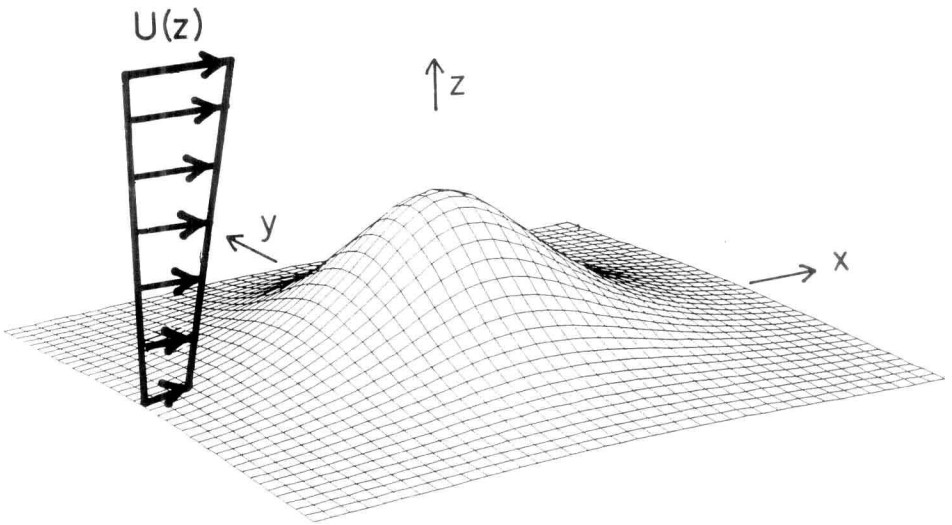

FIG. 1. Geometry of the mountain airflow problem with vertical exaggeration. The obstacle is specified by the function $h(x, y)$ and the incoming flow by $U(z)$, $\rho(z)$.

using standard notation (Batchelor, 1967). The flow variables—velocity $\mathbf{u}(x, y, z)$, pressure $p(x, y, z)$, and density $\rho(x, y, z)$—exist in the domain $-\infty < x, y < \infty$, $h \le z < \infty$, where $h(x, y)$ describes the irregular lower boundary (Fig. 1). The symbol ρ_0 represents a constant reference density. At the lower boundary, free-slip or no-slip conditions are specified for the velocity field and a no-flux condition for the density field. The inflow conditions $\mathbf{U}_H(z)$, $\rho(z)$, and $p(z)$ are assumed to be known. Disturbances produced by the obstacle are assumed to decay in the far field.

In the initial statement of the problem, Eqs. (1)–(3), the local time derivative has been retained in case the flow does not approach a steady state as anticipated as $t \to \infty$. The set (1)–(3) also includes viscous stress and mass diffusion to allow for the possibility that flows in the inviscid nondiffusive limit $\mu \to 0$, $\kappa \to 0$, differ from solutions with $\mu = \kappa = 0$ *a priori* (i.e., D'Alembert's paradox). Even vertical acceleration (Dw/Dt) is included in (1) as a starting point.

A set of idealized equations can be derived from (1)–(3) with the assumptions

$$\partial/\partial t = \mu = \kappa = 0 \tag{4}$$

and the ratio of the horizontal length scale L_H to vertical length scale L_z is large.

$$L_H/L_z \gg 1 \tag{5}$$

These are

$$\mathbf{u} \cdot \nabla \mathbf{u}_H = -\rho_0^{-1} \nabla_H p \tag{6}$$

$$\frac{\partial p}{\partial z} = -\rho g \tag{7}$$

$$\nabla \cdot \mathbf{u} = 0 \tag{8}$$

$$\mathbf{u} \cdot \nabla \rho = 0 \tag{9}$$

The effect of (5) is to reduce the vertical momentum equation, implicit in (1), to the statement of hydrostatic balance (7). The appropriate lower boundary condition for Eqs. (6)–(9) is

$$\mathbf{u} \cdot \mathbf{n} = 0, \qquad \text{on} \qquad z = h(x, y) \tag{10}$$

where $\mathbf{n}$ is the surface normal unit vector. As before, inflow conditions are assumed known, although in the two-dimensional (2-D) limit (i.e., flow over an infinite ridge), upstream influence of the ridge may have to be considered. On the top, lateral, and downstream boundaries, radiation or free-advection conditions might have to replace decay conditions due to the lack of dissipative mechanisms in Eqs. (6)–(9).

1.2. Conservation Laws

The idealized set (6)–(9) allows two conservation laws. Bernoulli's law,

$$\frac{1}{2}\rho_0 u^2 + p + \rho g z = \text{constant on a streamline} \tag{11}$$

where $u^2 = \mathbf{u} \cdot \mathbf{u}$, and the conservation of potential vorticity (PV),

$$\frac{D(PV)}{Dt} = 0 \tag{12}$$

where

$$PV = \frac{1}{\rho_0} \boldsymbol{\zeta} \cdot \nabla \rho \tag{13}$$

and $\boldsymbol{\zeta} = \nabla \times \mathbf{u}$. For cases with horizontally uniform incoming flow, (11) is constant on each entire density surface, and from (12), $PV = 0$ everywhere. This implies that all baroclinically produced vorticity exists as vectors tangent to density surfaces.

1.3. Scaling Laws

Due to the hydrostatic assumption (7), the scaling of (6)–(9) is particularly simple. First, no horizontal length scale arises in (6)–(9), except for that inherent in the hill shape $h(x, y)$. For particular inflow conditions, any solution to Eqs. (6)–(9), such as $p(x, y, z)$, is also a solution to the horizontally stretched problem $h = h(sx, sy)$, so $p = p(sx, sy, z)$, where s is an isotropic stretching factor.

Vertical scales in (6)–(9) arise from the mountain height and from the inflow functions $\mathbf{U}_H(z)$, $\rho(z)$. Excluding the case $\rho(z) = \text{constant}$, for which hydrostatic balance is not possible, the simplest inflow specification is

$$\mathbf{U}_H(z) = \mathbf{U}_0 = \text{constant}, \qquad \rho(z) = \rho_0\left(1 - \frac{N^2}{g}z\right) \tag{14}$$

where ρ_0, g, and N^2 are constants. Dimensional analysis then yields $L_z = U/N$, and a nondimensional mountain height $\hat{h} = h/L_z = hN/U$ arises as the only nondimensional control parameter in the problem, except for parameters needed to describe the mountain shape.

A linearly sheared inflow,

$$\mathbf{U}_H(z) = \mathbf{C}z + \mathbf{U}_0 \tag{15}$$

where $\mathbf{C} = C_x\mathbf{i} + C_y\mathbf{j}$ and $\mathbf{U}_0 = U_0\mathbf{i} + V_0\mathbf{j}$, provides vertical length scales $L_z = U_0/C_x$ and V_0/C_y. Two Richardson numbers, $Ri = (N/C_x)^2$ and $(N/C_y)^2$, arise as additional control parameters.

1.4. A Diagnostic Relation

It is useful to derive a diagnostic equation that relates flow speed to other variables, such as the field of vertical displacement $\eta(x, y, z)$. We suppose that there exists some pattern of density surface vertical displacement above the hill $\eta(x, y, z)$ which decays aloft (i.e., $\lim_{z\to\infty} \eta = 0$) and conforms to the hill [i.e., $\eta(x, y, z = h) = h(x, y)$]. This latter assumption, which is not strictly required in the following derivation, is inconsistent if a stagnation point exists on the surface $z = h$, allowing other density surfaces to intersect it.

Using (11) and following Sheppard (1956) by assuming hydrostatic balance far from the hill (7, 14), we can write Bernoulli's equation along a streamline as

$$u^2 = \frac{2}{\rho_0}\left(-p^* - \frac{1}{2}\rho_0 N^2\eta^2\right) + U_0^2 \tag{16}$$

where p^* is the difference between the pressure at a point (x, y, z) and the pressure at the same elevation far away (∞, ∞, z). Instead of making an assumption about p^*, as did Sheppard, we invoke the hydrostatic relation again to determine certain properties of p^* (Smith, 1988).

$$p^*(x, y, z) = g \int_z^\infty \rho' \, dz = \rho_0 N^2 \int_z^\infty \eta \, dz \tag{17}$$

where ρ' is the density anomaly. Because we want the lower limit of the integral (17) to lie on a particular density surface, it is convenient to write $\eta(x, y, z)$ in density coordinates: $\eta(x, y, z_0)$, where z_0 is the height of a particular density surface upstream, that is, $\rho = \rho(z_0)$.

With $dz = dz_0 + d\eta$, (17) becomes

$$p^*(x, y, z_0) = \rho_0 N^2 \left(I_\eta - \frac{1}{2} \eta^2 \right) \tag{18}$$

where

$$I_\eta(x, y, z_0) = \int_{z_0}^\infty \eta(x, y, z_0') \, dz_0' \tag{19}$$

Combining (16) and (18) gives

$$u^2 = -2N^2 I_\eta + U_0^2 \tag{20}$$

The canceling of the η^2 terms between (16) and (18) implies that speed variations predicted by (20) are associated only with nonlocal hydrostatic pressure variations and not with local parcel lifting. Stagnation (i.e., $u = 0$) begins when $I_\eta = U_0^2/2N^2$.

1.5. Early Results

By 1955, two major results concerning hydrostatic flow had been established for the case of 2-D flow over a ridge with constant $U_0 = U(z)$ and $N = N(z)$. First, Queney (1948) exhibited a solution to the linearized equations for flow over a Witch-of-Agnesi–shaped ridge (Fig. 2). (The Witch-of-Agnesi is a bell-shaped function described by the Italian mathematician Maria Agnesi in 1748 as a *versiera*, which translates correctly to *versed sine* but also to *witch*. This shape is commonly used in mathematical physics because of its simple Fourier transform.) Subsequent analysis by Eliassen and Palm (1960) and others showed that the concepts of group velocity, momentum and energy flux, and wave drag could be used to explain Queney's solution. The group velocity for 2-D standing hydrostatic gravity waves has a very special property: its direction is precisely vertical,

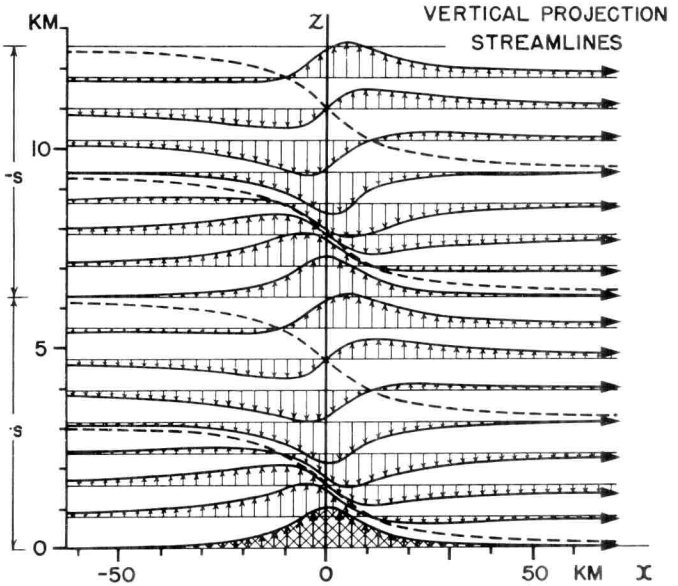

FIG. 2. Queney's (1948) linearized solution for hydrostatic airflow over a Witch-of-Agnesi shaped ridge. The steady pattern is composed of vertically propagating gravity waves which do not disperse.

independent of the horizontal wave number. Thus, the wave pattern does not disperse into its Fourier components as it propagates vertically. With the advent of satellite photography in the 1960s, observations of cirrus clouds produced by vertically propagating mountain waves verified these ideas. Figure 3 shows regions of cirrus starting abruptly at the position of three mountain ranges—Corsica-Sardinia, Apennines, and the Dinaric Alps—with no evidence of dispersive waviness.

The second important early result was the demonstration by Long (1953, 1955) that for a certain class of incoming flows and with a proper choice of dependent variables, the 2-D governing equation derived from Eqs. (6)–(9) becomes mathematically linear even for finite amplitude disturbances. The hydrostatic form of Long's equation is

$$\delta_{zz} + l^2\delta = 0 \tag{21}$$

where $l^2 = N^2/U_0^2$ and $\delta(x, z)$ is the field of vertical displacement from which the velocity fields $u(x, z)$ and $w(x, z)$ can be determined:

$$u = U_0(1 - \delta_z) \tag{22}$$

$$w = U_0\delta_x \tag{23}$$

FIG. 3. Mountain wave cirrus clouds generated by Corsica-Sardinia, the Italian Apennines, and the Yugoslavian coastal ranges. Such observations give evidence for vertical propagation without dispersion because they show only one line of high-level cloud generation for each mountain range, with little waviness.

Long showed that solutions to (21) in bounded regions would be realizable until closed or overturning streamlines developed, whereupon unsteady instabilities would occur. Solutions to (21) in an unbounded domain were later obtained by Huppert and Miles (1969).

Over the 20 years from 1955 to 1975, the literature on mountain waves continued to grow but attention remained centered on the 2-D linear theory and on Long's model solutions. Review papers and textbooks written during and immediately after this period reflect such a focus (Alaka, 1960; Nicholls, 1973; Long, 1972; Miles, 1969; Turner, 1973; Gill, 1982; Smith, 1979; GARP, 1980).

A broader attack on these problems began about 1975 and continues to the present day. Factors such as three-dimensionality, flow splitting, wave breaking, and wind reversals in the environment have been considered. The rapid progress in these areas has been due to the availability of high-speed computers for numerical simulation and to observational programs, especially ALPEX (the ALPine EXperiment), which stimulated and supported research on orographic effects. During the ALPEX field phase in 1982, few examples of simple, vertically propagating waves were found (Fig. 3 shows one). Instead, complicated flow phenomena such as flow splitting, shallow foehn, and bora with wind reversal aloft were more commonly seen (Smith, 1986a). These observations encouraged theoretical and numerical research into more realistic orographic flows.

The purpose here is to review the recent theoretical research on hydrostatic mountain flows and to construct a regime diagram displaying how the nature of the orographically disturbed flow depends on the control parameters of the problem.

2. Regimes of Flow

To organize this subject it is helpful to classify flow fields according to their kinematic character. On a parameter map, regimes are bounded by curves representing the onset of phenomena that alter the kinematic or geometric nature of the flow field. Two such phenomena are currently recognized: the onset of flow around instead of over a mountain (i.e., flow splitting) and the onset of wave breaking above the mountain. There is some parallelism between these two phenomena: each begins with the formation of a stagnation point, and each is associated with a recirculation region. Other phenomena, boundary layer separation for example, are not thought to be independent of the two mentioned, but the situation is unclear.

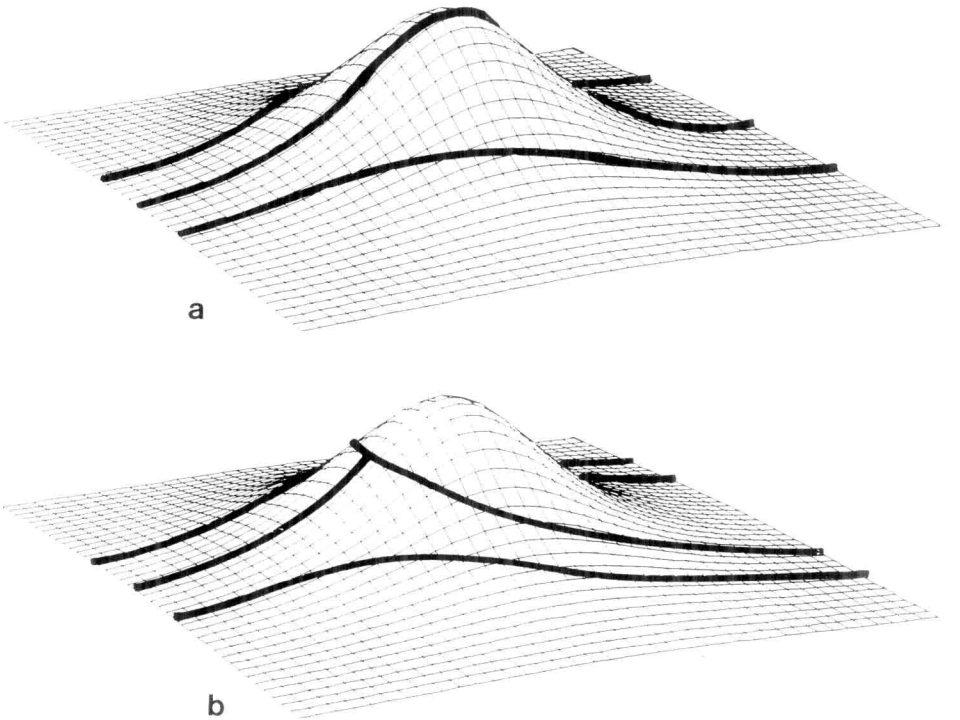

FIG. 4. Possible geometry of (a) nonsplit and (b) split flow past a hill. Split flow is characterized by the existence of a stagnation point at which streamlines can divide. Only streamlines that begin on the lower boundary are shown. The schematic does not include possible recirculation regions and wake eddies.

2.1. Flow Splitting

An essential feature of stratified flow past a hill is the selection of parcel trajectories over or around the hill (Fig. 4). This selection can be quantified as follows. For small isolated hills, $\hat{h} = hN/U \ll 1$, airflow tends to diverge around a hill, but the center streamline (for a hill with left-right symmetry or some other streamline if the hill shape is complex) is still able to climb over the hill top. For larger hills, a stagnation point can develop on the windward slope. At a stagnation point, the center streamline splits and passes around the hill on both sides. This splitting can only occur at a stagnation point because only there can the flow have two directions at one

point. The stagnation point also allows an upper density surface (or potential temperature surface in the atmosphere) to intersect the terrain, again by allowing the flow to be tangent to the lower boundary and tangent to the intersecting density surface at the same point. When flow splitting begins, the mountain-induced lifting is reduced and so is the amplitude of the gravity wave field aloft. If the flow field is continuous, a recirculation zone must exist just downstream of the stagnation point, with reversed flow at the surface.

2.2. Wave Breaking

A stagnation point can also form aloft. At such a point $u \ll U_0$, the streamlines become steeply sloping and overturning may follow, which is somewhat analogous to ocean waves breaking on a beach. The turbulence and dissipation associated with wave breaking can significantly alter the flow field everywhere, not just in the breaking region (Clark and Peltier, 1977). This is possible because internal gravity waves can communicate information about the breaking to other parts of the flow field.

2.3 Stagnation Points and a Regime Diagram

Both critical phenomena, flow splitting and wave breaking, depend on the formation of a stagnation point. It follows from the diagnostic equation (20) that stagnation does not depend on the local mountain height or slope but rather on the entire field of $\eta(x, y, z_0)$. Thus, estimating stagnation requires a full solution to the problem. Lacking an exact nonlinear solution for η, we temporarily use the approximate η field derived in Section 3 with the linearized governing equations to aid in the prediction of stagnation. An inconsistency in this method is apparent; the linearization must become locally invalid as stagnation approaches. We therefore view the results only as a first approximation.

According to linear theory (Smith, 1989), two particular regions in the flow have large values of I_η and are therefore candidates for early stagnation: one, a point above the hill at a nondimensional height of $\hat{z} \approx 4$; the other, a point on the windward slope of the hill. The former, being an interior maximum of I_η, occurs at a point where $\eta = 0$.

Figure 5 summarizes the onset of stagnation in an unstructured atmosphere (i.e., U_0 = constant and N = constant) as a function of the horizontal aspect ratio r of the hill and the nondimensional hill height $\hat{h}$. The family of

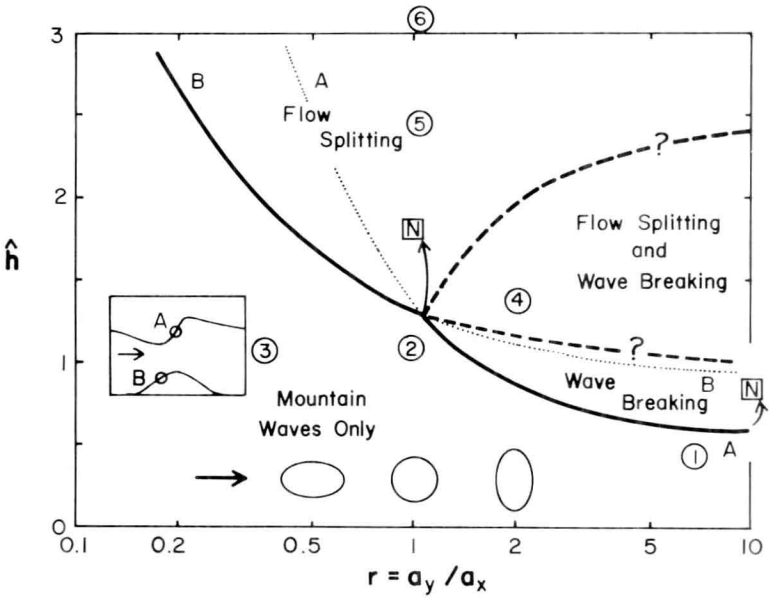

FIG. 5. Regime diagram for hydrostatic flow over a mountain. The diagram axes describe the mountain shape and size: r, the horizontal aspect ratio, and $\hat{h}$, the nondimensional mountain height. Solid curves A and B are linear theory estimates of flow stagnation (see Eqs. 20, 38, and 41), suggesting where wave breaking aloft (curve A) and flow splitting (curve B) will begin as $\hat{h}$ increases. The extensions of curves A and B (dotted lines) may be unphysical because the *first* appearance of a stagnation point could invalidate the linear theory estimates. The two boxes marked N indicate nonlinear calculations of stagnation and suggest that the linear theory prediction of critical mountain height may be about 30% too low. Other regime boundaries above the A and B curves (dashed) are not yet known. Numbered circles indicate Hawaiian Island parameters from Section 7, Table III. (Redrawn from Smith, 1989.)

hills considered in Fig. 5 is

$$h(x, y) = \frac{h_M}{[1 + (x/a_x)^2 + (y/a_y)^2]^n} \tag{24}$$

where the aspect ratio $r = a_y/a_x$ varies and $n = 3/2$. The diagram should be used by fixing a value of r and increasing $\hat{h}$ from a small value to a larger one until one of the critical curves is met. If curve A is met first, stagnation begins aloft. If curve B is met first, stagnation begins on the windward slope.

According to Fig. 5, stagnation begins aloft (curve A) for ridges with large aspect ratio, $r > 1$. This result is consistent with 2-D numerical

models that describe the onset of wave breaking aloft. Curve B above curve A is not believable because the influence of wave breaking is not considered in linear theory. Stagnation at the hill surface can occur, but a theory that includes wave breaking should be useful for predicting it (see Section 4).

For small aspect ratio, $r < 1$, stagnation begins on the windward slope (curve B). The stagnation point allows density surfaces to intersect the hill and flow splitting to occur. Curve A above curve B is not useful because the linear theory does not take into account the reduction in mountain wave amplitude associated with flow splitting. This amplitude-limiting process, together with the rapid dispersion of wave energy aloft, probably prevents wave breaking no matter how high the mountain is (Castro, 1987).

To the extent that the curves in Fig. 5 are accurate, they can be used to construct a regime diagram for hydrostatic flow. Three regions are seen:

1. Below the critical curves, gravity waves propagate vertically governed by the idealized set, Eqs. (6)–(9).
2. Above curve A (large $\hat{h}$ and r), wave breaking occurs.
3. Above curve B (large $\hat{h}$, small r), stagnation at the surface leads to flow splitting.

In addition, we must allow for

4. Combined wave breaking and flow splitting.

We refer to the final three of the four regimes as *nonideal* because the *a priori* assumptions of steady, inviscid, nondiffusive flow may not be valid, even in the limit of $t \to \infty$, $\mu \to 0$, and $\kappa \to 0$. The full set of equations (1)–(3), may be required.

The flow regimes in Fig. 5 are the basis for the organization of this review. Vertically propagating waves are analyzed in Section 3. Wave breaking and local hydraulics are discussed in Section 4. Ideas concerning flow splitting are presented in Section 5. Modifications to the regime diagram caused by vertical shear and vertical variations in static stability are described in Sections 6 and 7, respectively. A few applications to the earth's atmosphere are given in Section 8.

3. Mountain Waves

Two analytical methods are available for describing steady, vertically propagating gravity waves: linear theory and Long's Model (see Section 1.5). In the last ten years the primary advance has been the extension of

linear theory to three dimensions and the recasting of the theory into isentropic or density coordinates. Accordingly, we omit a detailed discussion of Long's model, referring the reader to earlier reviews (Miles, 1969; Long, 1972; Turner, 1973; Yih, 1965).

Vertical wave propagation has also been simulated with numerical models (Klemp and Lilly, 1978; Lilly and Klemp, 1979; Jusem and Barcilon, 1981; Clark and Peltier, 1977; Hoinka, 1985; Peltier and Clark, 1979, 1983; Pierrehumbert and Wyman, 1985; Rottman *et al.*, 1987). We omit a discussion of these numerical techniques but consider their results in Section 4.

3.1. Three-Dimensional Linear Theory in Isosteric Coordinates

The ideal set, Eqs. (6–9), can be rewritten in a new coordinate system (x, y, α), in which the specific volume α replaces z as the vertical coordinate.

Consider the set of equations governing inviscid, incompressible, hydrostatic fluid flow in isosteric coordinates (x, y, α):

$$D\mathbf{u}_H/Dt + \alpha\nabla_\alpha p + \nabla_\alpha\phi = 0 \tag{25}$$

$$D(\phi_\alpha)/Dt + \phi_\alpha\nabla_\alpha \cdot \mathbf{u}_H = 0 \tag{26}$$

$$\alpha\frac{\partial p}{\partial\alpha} + \frac{\partial\phi}{\partial\alpha} = 0 \tag{27}$$

where $\mathbf{u}_H = u\mathbf{i} + v\mathbf{j}$ is the horizontal velocity, p is the pressure, $\phi = gz$ is the geopotential, $\alpha = 1/\rho$ is the specific volume, and the total derivative operator is

$$\frac{D(\,)}{Dt} = \frac{\partial(\,)}{\partial t} + \mathbf{u}_H \cdot \nabla_\alpha(\,) \tag{28}$$

The subscript on the del operator in (25)–(28) implies holding α constant whereas the subscript on a variable implies differentiation with respect to α. The coordinate system (x, y, α) is not precisely orthogonal due to the tilt of the density surfaces, but the off-diagonal metric coefficients that the tilt introduces into the transformation are neglected as being no larger than the previously neglected nonhydrostatic effects (Pielke, 1984). The advantages of this coordinate system are several. First, as long as the low-level flow goes over the hill (assumed in this section), the lower boundary condition can be applied on a coordinate surface:

$$\phi(\alpha = \alpha_0) = gh(x, y) \tag{29}$$

Second, the conservation laws (11) and (12) are more easily applied in isosteric coordinates, simplifying the flow diagnosis. Bernoulli's function is